Available online at www.sciencedirect.com

SciVerse ScienceDirect

Ceramics International 39 (2013) 1485–1493

CERAMICS INTERNATIONAL

www.elsevier.com/locate/ceramint

Non-stirred synthesis of Na- and Mg-doped, carbonated apatitic calcium phosphate

Preston R. Larson[a], Andrew S. Madden[b], A. Cuneyt Tas[c,*]

[a]Samuel Roberts Noble Electron Microscopy Laboratory, University of Oklahoma, Norman, OK 73019, USA
[b]School of Geology and Geophysics, University of Oklahoma, Norman, OK 73019, USA
[c]College of Dentistry, University of Oklahoma Health Sciences Center, Oklahoma City, OK 73117, USA

Received 22 June 2012; received in revised form 28 July 2012; accepted 28 July 2012
Available online 15 August 2012

Abstract

Hydroxyapatite-like (apatitic) calcium phosphate (Ap-CaP) powders are usually synthesized in stirred solutions containing the highly soluble salts of calcium, such as calcium nitrate, calcium acetate and calcium chloride as the Ca-source. The current study tested the ideas of simultaneously using (i) precipitated calcite ($CaCO_3$) powders as the Ca-source and (ii) non-stirred, static solutions for synthesizing carbonated, Na^+- and Mg^{2+}-doped apatitic calcium phosphate (Ap-CaP) powders. 0.5 M phosphate buffer (non-saline) solutions were used as the sole phosphate source. The synthesized Ap-CaP powders were found to consist of micron-size carnation-like crystalline particles. Samples were characterized by FE-SEM, XRD, FTIR, ICP-AES, dynamic light scattering (DLS), carbon percentage and BET surface area analyses.

Keywords: Apatite; Calcite; Non-stirred; Synthesis

1. Introduction

The inorganic portion of bones consists of a carbonated, ionically-substituted, non-stoichiometric, cryptocrystalline and apatitic calcium phosphate phase having only slight resemblance to the stoichiometric compound calcium hydroxyapatite (HA, $Ca_{10}(PO_4)_6(OH)_2$) [1,2]. Materials chemists usually strive to develop synthesis methods which can produce apatitic calcium phosphate similar to bone mineral rather than stoichiometric calcium hydroxyapatite. To that end the accurate elemental analysis of bone and tooth specimens recently given by Castro [3] could be a useful starting point. Briefly, human bones contain 24.5 wt% Ca^{2+}, 11.5% P, 5.8% CO_3^{2-}, 0.7% Na^+, 0.55% Mg^{2+}, and 0.03% K^+, besides a number of trace elements at the ppm level including Zn^{2+}, Fe^{3+}, Sr^{2+}, Pb^{2+}, Ba^{2+}, Cu^{2+}, *etc.* [2,3]. Carbonate, sodium, and magnesium ions are the major dopants of apatitic (apatite-like) calcium phosphate (Ap-CaP) bone mineral. Bone mineral, which undergoes a maturation period measured by years (both prenatal and childhood), does not contain phases such as α- or β-$Ca_3(PO_4)_2$, $Ca_8(HPO_4)_2(PO_4)_4 \cdot 5H_2O$, $Ca(H_2PO_4)_2 \cdot H_2O$, $CaHPO_4 \cdot 2H_2O$, or $CaHPO_4$, mainly because all of these are not thermodynamically stable in physiological fluids.

Ap-CaP bioceramics find uses in the manufacture of synthetic hard tissue repair biomaterials, dense or porous scaffolds, self-setting orthopedic or dental cements, and as drug-, biomolecule- or growth factor-delivery agents [4]. Alkali and alkaline earth ion-doped, carbonated, high surface area ($> 160\ m^2/g$) and nanosize (< 30 nm) apatitic calcium phosphate powders were biomimetically produced by using synthetic body fluid solutions (SBF) as the synthesis medium [5–8]. Nevertheless, one needs to be careful about (*i*) not introducing anions (such as nitrate, ammonium or acetate) which are not present in human blood into such so-called biomimetic syntheses and (*ii*) not contaminating the product with such foreign anions even at low levels, as shown by Ivanova *et al.* [9]. Previous biomimetic syntheses were unfortunately performed in the presence of significant amounts of nitrate, chloride and ammonium ions [5–8,10,11].

*Corresponding author. Tel.: +1 979 633 8064.
E-mail address: c_tas@hotmail.com (A.C. Tas).
URL: http://www.cuneyttas.com (A.C. Tas).

0272-8842/$ - see front matter © 2012 Elsevier Ltd and Techna Group S.r.l. All rights reserved.
http://dx.doi.org/10.1016/j.ceramint.2012.07.095

Powders of Ap-CaP bioceramics were usually synthesized in well-agitated, stirred solutions, since the early works of Hayek *et al.* [12–14]. The classical recipes [12–17] for apatite synthesis typically used a solution pH at or above 10.5 by adding aliquots of strong bases (NH_4OH, NaOH or KOH), although physiological fluids, in which the biological systems produce biological Ap-CaP, are not alkaline solutions. Stirred synthesis reactors would of course enhance the reaction rates. However, biological and geological systems do not use stir bars, stir rods or electrical stirrers in crystallizing carbonated calcium phosphates or calcium carbonates.

Non-stirred synthesis of CaP bioceramics has not received much attention until now. The need for studying and developing non-stirred, non-agitated Ap-CaP synthesis/biomineralization processes arises if immersing a biopolymer-based (such as made out of collagen, properly cross-linked gelatin, chitin, cellulose, alginate, glycan, demineralized bone matrix, *etc.*) nano-fibrous mat, mesh or membrane directly into the biomineralization/synthesis media becomes necessary. In this case stirring the biomineralization media could easily destroy the fragile biopolymer membranes.

We have recently reported on the formation of brushite ($CaHPO_4 \cdot 2H_2O$) crystallized with a unique spherical micro-granule morphology in a non-stirred, completely static crystallization process, free of organics, using precipitated $CaCO_3$ (calcite) powder as the only calcium source [18]. The current study on carbonated, alkali and alkaline earth ion doped Ap-CaP production may be regarded as a variant of our recent attempt [18] on non-stirred brushite synthesis. Within our broader pursuit of the inexpensive, large-scale and non-stirred crystallization processes in the $CaO–P_2O_5–H_2O$ system, the present study was aimed at developing a synthesis procedure to simultaneously satisfy the following engineering criteria:

(i) to facilitate the large-scale production of Na- and Mg-doped, carbonated Ap-CaP at pH 7 in non-stirred glass vessels,
(ii) to have a synthesis process which would not need any pH control,
(iii) to have reaction temperatures high enough (60–70 °C) to minimize the risk of bacteria growth in the solutions, without a need to add sodium azide (NaN_3) or other similar antimicrobial toxic chemicals,
(iv) to use commercially available, inexpensive, precipitated $CaCO_3$ powder contaminated with ppm level magnesium as the sole source of calcium, magnesium and carbonate ions,
(v) to use soluble sodium phosphate salts as the only source of sodium and hydrogen phosphate ions, and
(vi) to have synthesis solutions which are completely free of foreign ions such as nitrate, chloride, acetate and ammonium.

The main emphasis in this study was placed on reporting the particle morphology of these new Ap-CaP powders and determining compositions by quantitative chemical analyses.

Historically, the interest in the conversion of $CaCO_3$ into Ap-CaP, to obtain porous biomaterials, started with the pioneering work of Della M. Roy in the early 70s [19–21]. In those studies, Roy *et al.* [20,21] investigated the conversion of natural coral skeletal aragonite (*Porites*) by using high temperatures (140–260 °C) and high autoclave pressures (550–1055 kg/cm^2) in the presence of acidic (such as, $CaHPO_4$ and $Ca(H_2PO_4)_2 \cdot H_2O$) and basic (such as, $(NH_4)_2HPO_4$) phosphates, as well as sodium or potassium orthophosphates and acetic acid. Hydrothermal reactions were carried out in agitated autoclaves from 12 to 48 h under the above-mentioned experimental conditions.

Over the last four decades, these early studies of Roy *et al.* [19–21] have been significantly duplicated, modified, or used as inspiration for other work. The literature on these attempts is immense, but just to name a few examples, the works of Zaremba *et al.* [22], Su *et al.* [23], Ni and Ratner [24], and Jinawath *et al.* [25] could be cited. Nowadays, converted coral and other marine skeletal species are also available as commercial, clinical porous bone graft biomaterials [26,27]. However, in most coral or marine species the major starting phase was biological aragonite, and its conversion to Ap-CaP was more difficult than that of the calcite ($CaCO_3$) used in the current study as those previous experiments needed higher temperatures, and more importantly, higher pressures to convert biological aragonite to Ap-CaP [19–25]. Experimental studies only using calcite powders and producing macroporous or non-porous Ap-CaP biomedical scaffolds from those were rare [28].

2. Materials and methods

2.1. Materials

Calcium carbonate powder (> 99%, $CaCO_3$, Fisher Scientific, Fair Lawn, NJ, Catalog no.: C63, Chalk, precipitated), Na_2HPO_4 (> 99.9%, disodium hydrogen phosphate anhydrous, Fisher Scientific, Catalog no.: S375) and NaH_2PO_4 (> 99.9%, sodium dihydrogen phosphate anhydrous, Sigma-Aldrich, St. Louis, MO, Catalog no.: S0751) were used during syntheses. Freshly boiled (to remove any dissolved bicarbonate ions originating from the contact with laboratory atmosphere) de-ionized water (18.2 MΩ) was used in all experiments. Reactions were performed in heat-sterilized (140 °C, 8 h) and unused Pyrex® glass media bottles.

2.2. Solution preparation and powder synthesis

0.5 M phosphate buffer solution of pH 7 was prepared as follows; 1000 mL of pre-boiled, de-ionized water was placed in a 1 L-capacity beaker, followed by adding 49.686 g of Na_2HPO_4 (=0.35 M HPO_4^{2-}) and stirring at room temperature (RT, 22 ± 0.5 °C). 17.997 g of NaH_2PO_4

(=0.15 M $H_2PO_4^-$) was then added to obtain a solution with pH 7 at RT. Commercially available phosphate buffer saline (PBS) solutions were not used in this study to have synthesis media free of Cl^- ions.

To synthesize Na- and Mg-doped, carbonated Ap-CaP powders, 1 L of this freshly prepared solution was placed into a 1 L-capacity glass media bottle containing 20.00 g of precipitated $CaCO_3$ powder. The glass media bottle was closed by using its plastic screw cap and placed into an oven at 70 ± 0.2 °C. The bottles were kept undisturbed in the oven for 24, 48 and 72 h. 48- and 72 h-bottles were replenished (by carefully decanting the used solutions) by freshly prepared 0.5 M phosphate buffer solutions at the end of every 24 h. At the end of the above-stated holding times at 70 °C, solids were separated from their mother liquors by using filter paper, washed with ample amount of deionized water, and dried in clean watch glasses at 35 °C for 48 h in a pre-sterilized box oven in an air atmosphere. Some synthesis experiments were also performed similarly at 60 °C.

2.3. Sample characterization

Prior to powder X-ray diffraction (XRD) and Fourier-transform infrared spectroscopy (FTIR) analyses, the dried samples were manually ground in an agate mortar by using an agate pestle. XRD runs were performed (Advance D8, Bruker, Karlsruhe, Germany and Ultima IV, Rigaku, Tokyo, Japan) in the step scan mode, with a step size of 0.03° and preset time of 3 s. The powder diffractometer was equipped with a Cu tube and operated at 40 kV and 40 mA. XRD samples were prepared by gently packing the powders into the sample holder cavity around 1 mm-deep.

FTIR samples were mixed with KBr powders at the ratio of 1 mg sample-to-250 mg KBr in an agate mortar. FTIR pellets with a diameter of 12.5 mm were pressed at a load of 10 metric ton for 1 min. FTIR data were collected (Spectrum One, PerkinElmer, Waltham, MA) by using 256 scans.

Samples for field emission-scanning electron microscopy (Zeiss-Neon 40 EsB, Oberkochen, Germany and Hitachi-S4800, Tokyo, Japan) were not ground and the small sample chunks embedded on carbon sticky tapes were sputter-coated with a thin layer of gold–palladium prior to imaging at 5 kV with a working distance of 6 mm. Chemical analyses of powder samples were performed by using inductively-coupled plasma atomic emission spectroscopy (ICP-AES, Model 61E, Thermo Electron, Madison, WI). For the ICP-AES analyses, 75 mg portions of powder samples were dissolved in 5 mL of concentrated HNO_3 solution.

The BET surface area of powder samples was determined by applying the standard Brunnauer–Emmet–Teller method to the nitrogen adsorption isotherm obtained at −196 °C using either a Micromeritics ASAP 2020 (Norcross, GA) or Quantachrome, Nova 2000e (Boynton Beach, FL) instrument. Thermogravimetric/differential thermal analyses (TG/DTA, Model 851e, Mettler-Toledo, Columbus, OH) of the starting $CaCO_3$ powders were performed in Pt crucibles in a static air atmosphere with a heating rate of 5 °C/min from RT to 1150 °C. Al_2O_3 powder was used as a reference sample in the DTA experiments. Particle size analyses were performed at RT by using dynamic light scattering (DLS; ZetaSizer NS, Malvern Instruments Ltd., Worcestershire, UK). 50 mg of powder samples were placed in small glass bottles having 25 mL of deionized water and then manually shaken for 2 min. Ultrasonification or physical milling was not used in order not to damage or disintegrate the original micron-size particles of this study. The average of three DLS runs (15 s each) was used in reporting the particle sizes.

3. Results and discussion

$CaCO_3$ powders (Fisher Scientific, Catalog no. C63) of this study were of calcite form. The XRD pattern (Fig. 1a) of these powders matched well with that presented in the ICDD-PDF (*International Centre for Diffraction Data-Powder Diffraction File*) 05-0586 for calcite. The lattice parameters of the calcite powder of Fig. 1a were found to be $a=0.4999$ nm, $c=1.7062$ nm, $\alpha=\beta=90°$, $\gamma=120°$, $Z=6$.

The characteristic FTIR spectrum of these $CaCO_3$ powders is given in Fig. 1b. The three carbonate group vibration bands, namely, v_3 (asymmetric stretching, 1400 cm^{-1}), v_2-0 and v_2-2 (out-of-plane bending, 848 and 873 cm^{-1}), and v_4-2 (in-plane bending, 713 cm^{-1}) are visible [29]. The particle morphology of the calcite powders is depicted in Fig. 1c. Calcite particles were comprised of significantly agglomerated or inter-grown submicron spindles (as shown in the inset of Fig. 1c). It would not be appropriate to report a single value for the mean particle size when working with such powders agglomerated at the submicron level.

The BET surface area of the $CaCO_3$ powders was 6 m^2/g and the TG/DTA data for these powders are shown in Fig. 1d. The calcium carbonate powder of this study started to decompose into CaO at 665 °C and the decomposition was completed when the temperature reached 800 °C (at 5 °C/min heating rate in an ambient air atmosphere). That 56.45% (% weight remained) noted on the TG trace simultaneously corresponded to 43.55% (=100–56.45) total weight loss. The theoretical weight loss for the complete decomposition of $CaCO_3$ into CaO is 43.97%. The discrepancy of about 0.4% between the theoretical and the actual weight loss percentage is considered to be within the experimental error margin of our TG runs. The inset of Fig. 1d shows the DTA signal plotted over the temperature range of 600–1000 °C, clearly indicating an endothermic peak for this decomposition reaction. TG/DTA experiments, yielding the start and finish temperatures of the $CaCO_3$-to-CaO conversion in air, are especially useful in comparing different calcite samples of different origin and purity with one another [30–32]. Readers of this article who would like to reproduce the

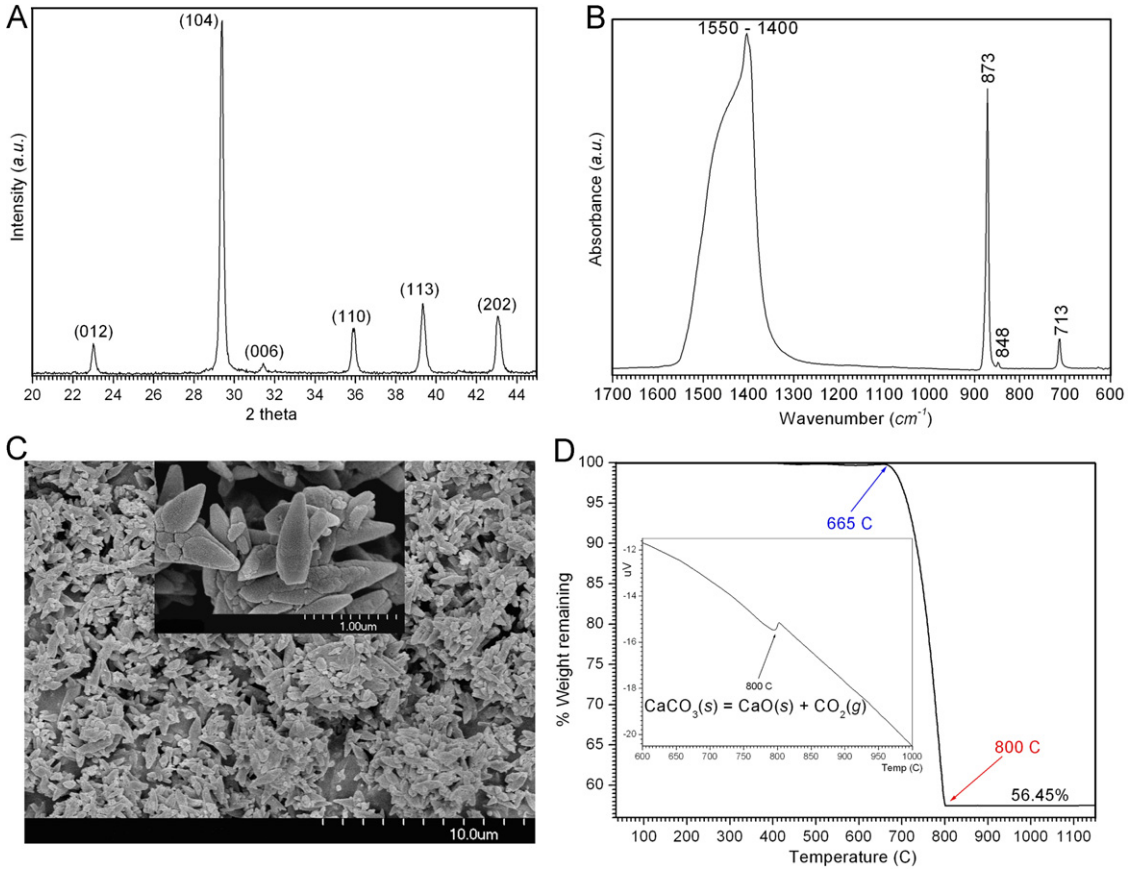

Fig. 1. (a) XRD data of $CaCO_3$ powders, (b) FTIR data of $CaCO_3$ powders, (c) Particle morphology of $CaCO_3$ powders and (d) TG and DTA data of $CaCO_3$ powders.

synthesis process described here are advised to use a $CaCO_3$ powder with similar physicochemical properties to ours.

$CaCO_3$ powders were found to have 2410 ± 35 ppm Mg, 335 ± 14 ppm Fe, 295 ± 10 ppm K, 304 ± 12 ppm S, 98 ± 7 ppm P, 75 ± 11 ppm Na, 24 ± 3 ppm Mn, 17 ± 3 ppm Zn, and 39.7 wt% Ca according to the ICP-AES analyses. The magnesium already present in these powders was useful in synthesizing Mg-doped Ap-CaP by using these powders, and for this reason no Mg was added to the synthesis solutions. Precipitated $CaCO_3$ powders are usually produced by the carbonation process of $Ca(OH)_2$ suspensions [33,34], and the ppm-level impurities (such as Mg, Fe, Mn, S, Zn, K, *etc.*) of natural origin present in the $Ca(OH)_2$ used in these processes would thus be detected in the synthesized $CaCO_3$ powders.

Carbonated, Na- and Mg-doped Ap-CaP powders were produced by using the above-mentioned $CaCO_3$ powders. The particles of Ap-CaP had a carnation-like (*Dianthus caryophyllus* or clove pink) shape. The SEM images given in Fig. 2 depicted the particles of Ap-CaP powders obtained by soaking $CaCO_3$ powders in non-stirred 0.5 M phosphate buffer solutions at 60 °C (for 24 and 48 h) and 70 °C (72 h). This particle morphology was not reported before for hydroxyapatite since such powders were typically synthesized in stirred reactors. Nevertheless, the carnation-like morphology shown in Fig. 2 bears some resemblance to the carbonated and Mg-doped Ap-CaP precipitates in situ crystallizing in non-stirred, supersaturated calcium phosphate (*i.e.*, SBF) solutions heated to 37 °C; see Tables II and III of Ref. [35] and Fig. 5 of Ref. [36]. All micrographs of Fig. 2 showed no $CaCO_3$ particles similar to those shown in Fig. 1c. The image of the "24 h-at-60 °C" sample captured in Fig. 2b shows the early stages of the carnation-like Ap-CaP particle formation, where the individual interlocking platelets were not yet fully dense and the platelet surfaces were not smooth. However, in the micrograph of the "48 h-at-60 °C" sample (Fig. 2d), the platelets were dense (free of any voids visible in Fig. 2b), their edges are slightly jagged, but their surfaces were smooth. The interlocked platelets of Fig. 2d had a thickness of 17 ± 8 nm (directly measured from the SEM images). The platelets of the "72 h-at-70 °C" sample (Fig. 2f) were more uniform in thickness (25 ± 3 nm) and their edges were less jagged in comparison to those of Fig. 2d.

The results of particle size analyses performed by dynamic light scattering indicated the carnation-like Ap-CaP powders had an average particle size of about 7 ± 2 μm (Fig. 3). The peaks observed in Fig. 3 corresponded to 100% of the volume for each sample. Aqueous synthesis methods which are suitable for the production of

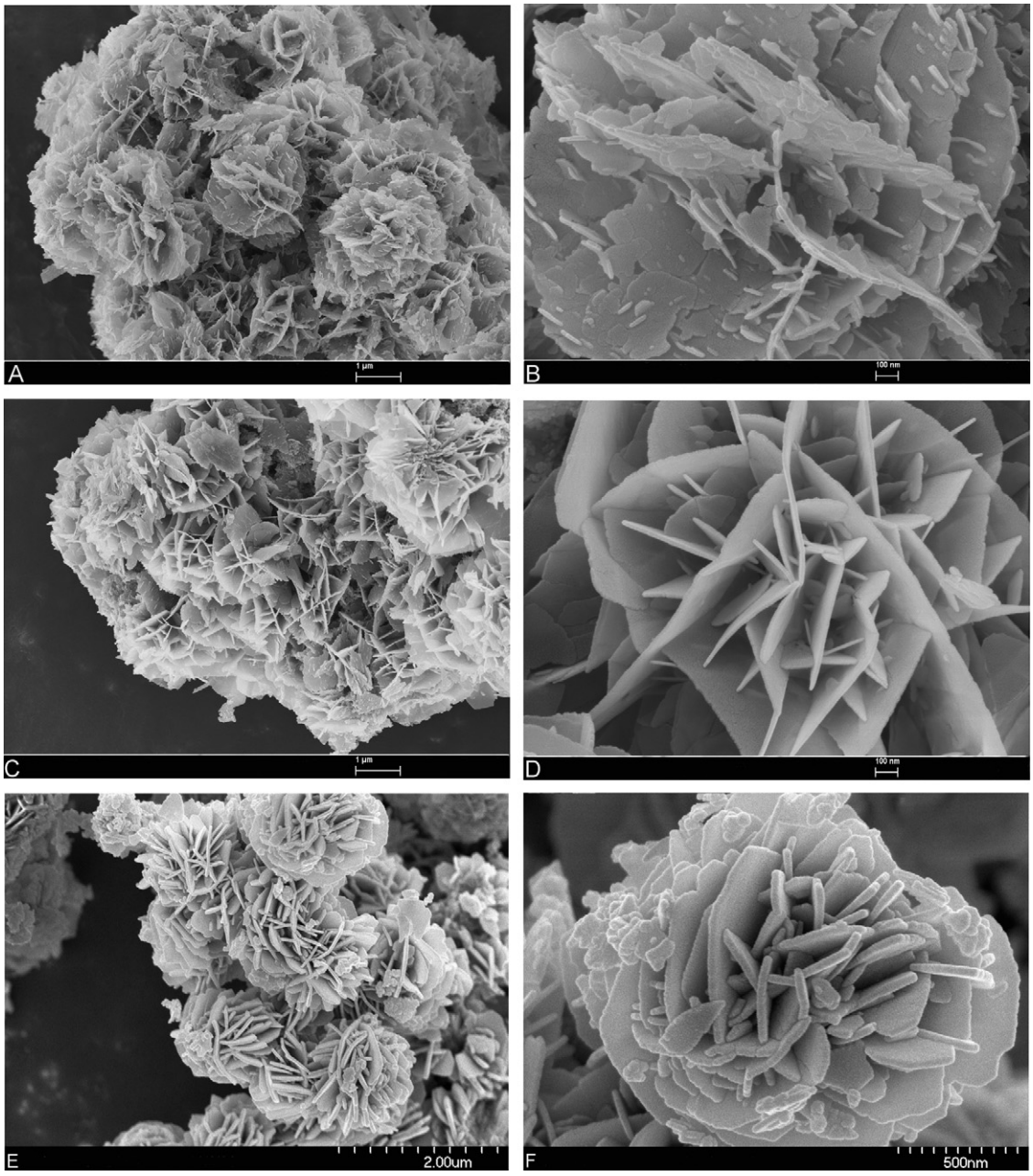

Fig. 2. SEM photomicrographs of Ap-CaP powders obtained by soaking precipitated $CaCO_3$ in 0.5 M phosphate buffer solution at (a) and (b) 60 °C for 24 h, (c) and (d) 60 °C for 48 h, (e) and (f) 70 °C for 72 h.

Ap-CaP powders having such large particle sizes are not abundant in the previous literature.

The powder XRD data of solids recovered from the non-stirred 0.5 M phosphate buffer solutions after 24 and 48 h at 60 °C are given in Fig. 4a, whereas those obtained from 24, 48 and 72 h at 70 °C are reproduced in Fig. 4b. The vertical dashed lines in both Fig. 4a and b indicate the theoretical position (29.415° in ICDD PDF 05-0586) of the most intense (104) reflection of pure calcite along the 2θ axis. Based on the data of Fig. 4a and b, 24 h samples (both at 60 and 70 °C) contained a noticeable amount of non-reacted calcite, but for the 48 and 72 h samples that amount decreased to levels below the detection limit of the XRD scans. The inset of Fig. 4a shows the FTIR data of "24 h-at-60 °C" samples. All peaks in the 48 h (60 and 70 °C) and 72 h (70 °C) XRD traces of Fig. 4 belonged to apatitic calcium phosphate (Ap-CaP), which can be matched by the ICDD PDF 09-0432. The two insets in Fig. 4b confirmed that the "72 h-at-70 °C" sample was single-phase Ap-CaP (all peaks corresponding to those of ICDD PDF 09-0432), with lattice parameters, $a=9.418$, $c=6.884$ Å, and it was free of any $Ca_8(HPO_4)_2(PO_4)_4 \cdot 5H_2O$ (octacalcium phosphate, OCP) phase. If OCP was present, its (010) reflection would have been detected at 4.72° 2θ (ICDD PDF 26-1056) in the second inset of Fig. 4b. OCP is, nevertheless, known to be not stable in aqueous media of pH 7 [37].

The characteristic FTIR spectrum of the "72 h-at-70 °C" sample is shown in Fig. 4c. Since the sharp and strong OH^- band observed at 3571 cm^{-1}, for stoichiometric calcium hydroxyapatite ($Ca_{10}(PO_4)_6(OH)_2$), is absent, such hydroxyl ion-deficient samples could only be named as apatitic calcium phosphates (Ap-CaP). Loong *et al.* [38] have shown that the mineral portion of the newly formed bone tissues was OH-deficient.

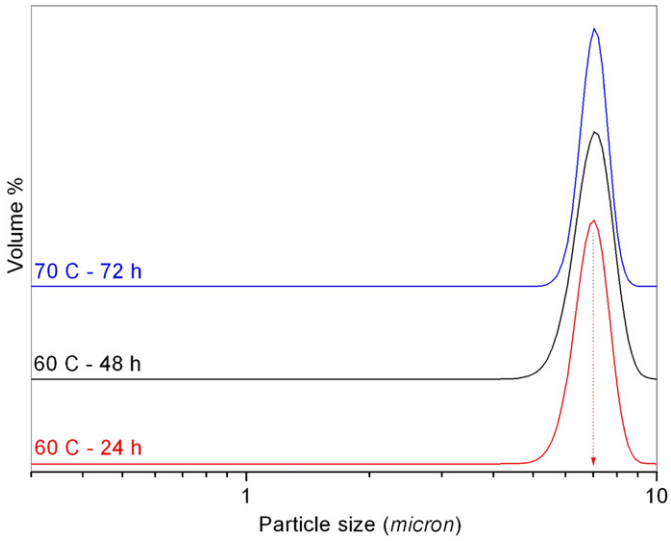

Fig. 3. Particle size distribution of powders by dynamic light scattering (DLS) measurements.

Carbonate ions (CO_3^{2-}) can occupy two different crystallographic sites in the unit cell of stoichiometric Ca-hydroxyapatite (hexagonal, space group $P6_3/m$); one is occupied by OH and located along the unit cell edges, as shown in Fig. 4d, and the other is occupied by PO_4 (within the unit cell). These two sites for CO_3^{2-} substitution are called the A site and B site, respectively [39].

If, for instance, all the hydroxyl ions present in the A site were replaced by CO_3^{2-}, then the mineral would be called dahllite ($Ca_{10}(PO_4)_6CO_3$ or $CaCO_3 \cdot 3Ca_3(PO_4)_2$), having a pseudo-hexagonal unit cell ($\gamma = 120.36°$) of monoclinic space group P*b* [40,41]. According to its formula, dahllite has a CO_3^{2-} content of 5.82 wt%. A-type carbonate apatites (*i.e.*, dahllite) with almost complete replacement of OH^- with CO_3^{2-} were produced by heating stoichiometric HA in a very dry CO_2 atmosphere at temperatures in excess of 950 °C for about 72 h [42], therefore, the synthesis of fully A-type carbonated apatites in aqueous solutions is expected to be difficult if not impossible.

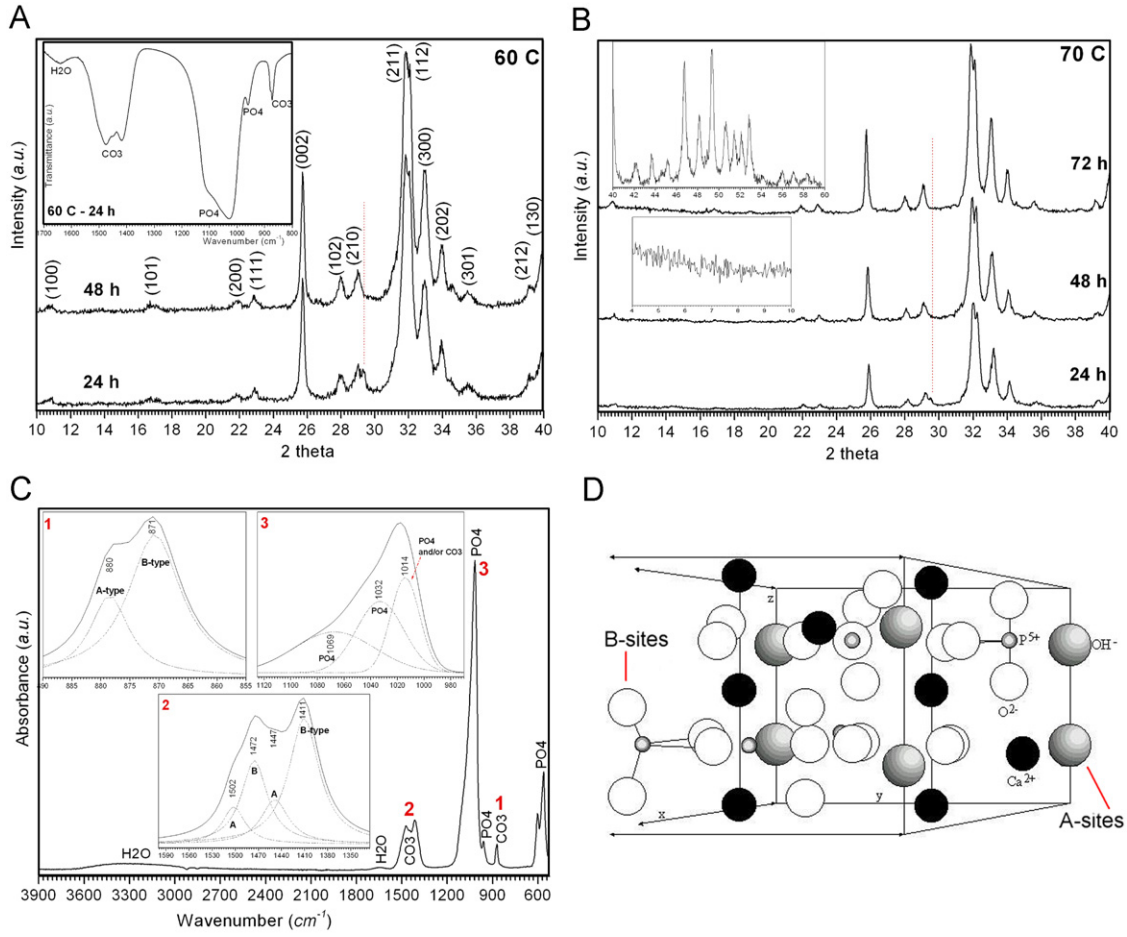

Fig. 4. (a) XRD data of Ap-CaP powders synthesized at 60 °C (soaking times are indicated on the data traces; inset shows the FTIR data of 60 °C–24 h samples), (b) XRD data of Ap-CaP powders synthesized at 70 °C (the two insets showing XRD data over the 4–10° 2θ and 40–55° 2θ ranges for the "72 h-at-70 °C" sample), (c) FTIR data of 72 h-at-70 °C sample (*Ap-CaP*); insets showing the de-convoluted IR bands for A- and B-type CO_3^{2-} substitutions and (d) Unit cell of stoichiometric apatite (A- and B-sites for CO_3^{2-} replacement are indicated).

On the other hand, the substitution of the trivalent PO_4^{3-} ion of the apatitic unit cell by the bivalent CO_3^{2-} ion is named as B-type carbonate substitution. If there were 5 PO_4^{3-} and 1 CO_3^{2-} ions at the B-sites of the unit cell, then to maintain the electroneutrality of the lattice one Ca^{2+} vacancy and one OH^- vacancy (the A-sites) would be created, and the resultant B-type carbonated Ap-CaP would have the formula of $Ca_9(PO_4)_5(CO_3)(OH)$, with a theoretical CO_3^{2-} content of 6.576 wt%.

However, as indicated by previous studies [38,43], the bone mineral is hydroxyl-deficient and Na-doped so that the above simplified formula is not sufficient to describe the more complex and extensively carbonated (5.8 wt%) bone mineral. CO_3^{2-} and Na^+ substitutions would simultaneously cause the dehydroxylation of the Ap-CaP lattice, and this is why we did not observe the sharp OH^- band at 3571 cm^{-1} in Fig. 4c, as is the case with the bone mineral [43].

Sodium (Na^+)-substituted B-type apatitic CaP can be described by the chemical formula $Ca_{10-x-y}Na_x(V_{Ca})_y(PO_4)_{6-x}(CO_3)_x(OH)_{2-y/2}(V_{OH})_{y/2}$, where V denoted the vacancies created at the Ca and OH sites [44,45]. On the other hand, mixed A- and B-type CO_3^{2-} substitution, which takes place according to $Ca_{10-x}(PO_4)_{6-x}(CO_3)_x(OH)_{2-x-2y}(CO_3)_y$, is usually seen in solution synthesized Ap-CaP powders [39,46–48].

The previous literature usually underestimated the significance of deconvoluting the peaks of FTIR data to determine the type of CO_3^{2-} substitutions taking place in the solution synthesized Ap-CaP powders [5,6,44,49]. The insets in Fig. 4c depicted the deconvolution of the important IR peaks of the bottom IR trace and thus confirmed that the Ap-CaP powders of the current study were having simultaneous A- and B-type CO_3^{2-} substitutions [45,50–53]. An ample supply of HCO_3^- ions was provided to our synthesis solutions by the selection of precipitated $CaCO_3$ as the starting material.

The results of the ICP-AES, carbon%, BET surface area (and DLS) analyses of the washed and RT-dried Ap-CaP precipitates are given in Table 1. The Ca/P molar ratio of the bone mineral is close to 1.70 [38]. The Ca/P molar ratios of the Ap-CaP samples synthesized at 70 °C do not show significant Ca-deficiency with respect to the bone mineral. The significant amount of Na-doping (2–3 wt%) into the solids is due to the use of 0.5 M sodium phosphate buffer (non-saline) solutions. Mg-doping (of about 2000 ppm) into the Ap-CaP samples was also achieved. Carbonate percentages (Table 1) of the Ap-CaP samples synthesized at 70 °C were quite close to that of the bone mineral, *i.e.*, 5.8 wt% [2–4,35]. According to the ICP-AES data, the tentative formula of the "72 h-at-70 °C" samples of this study could be given as $Ca_{8.875}Na_{1.25}(PO_4)_{5.733}(CO_3)_{0.9}$. This formula has the drawback of not accounting for any of the lattice OH^- ions (which do not show up in the FTIR data of Fig. 4c) that may still be present in the Ap-CaP powders.

This study showed that the carbonated (very close to the carbonate content of human bone mineral), Na-and Mg-doped carnation-like Ap-CaP powders could be produced in non-stirred, nitrate-, acetate-, chloride-, ammonium- and organics-free solutions at temperatures of 60 and 70 °C. Previous studies [54–56] also produced flower-like Ap-CaP particles at temperatures higher than 70 °C but their synthesis procedures were unfortunately not free of ions (such as NH_4^+, NO_3^-, Cl^-, *etc.*) and organic substances (ethylenediaminetetraacetic acid, *EDTA*, sodium dodecyl sulphate, *SDS*, and ethylene glycol, *EG*) foreign to the human metabolism. The BET surface areas of the powders decreased in accord with increasing temperature and time of crystallization. The decrease in the experimentally measured BET surface areas coincided with the change in particle morphology depicted in Fig. 2b, d and f, respectively. The "48 h-at-60 °C" samples with a respectably high surface area of 56 m^2/g could be suitable for use in numerous dental (*e.g.*, pulp capping) and orthopedic (*e.g.*, bone cement preparation) applications.

4. Conclusions

Precipitated calcite ($CaCO_3$) can be used as the only Ca-source in the large-scale synthesis of carbonated, Na^+- and Mg^{2+}-doped apatitic calcium phosphate (Ap-CaP) powders in non-stirred 0.5 M phosphate buffer (non-saline) solutions in 48 or 72 h at either 60 or 70 °C. The synthesized Ap-CaP powders, with BET surface areas over the range of 35–65 m^2/g, consisted of micron-size carnation-like crystalline particles. The synthesis procedure presented here avoided contamination of the resultant powders with nitrate, acetate, ammonium or chloride ions.

Table 1
Results of the ICP-AES, %carbon, BET, and DLS analyses*.

Solid samples	%Ca	%P	Ca/P molar	%Na	%Mg	%C	$\%CO_3$	BET (m^2/g)	Particle size (μm)
60 °C–24 h	–	–	–	–	–	–	–	65	7.2 ± 1.9
60 °C–48 h	–	–	–	–	–	–	–	56	7.3 ± 2
70 °C–24 h	34.82	15.82	1.70	2.27	0.22	1.07	5.34	57	–
70 °C–48 h	32.70	15.30	1.65	2.52	0.21	1.09	5.45	43	–
70 °C–72 h	36.09	16.84	1.66	2.96	0.22	1.11	5.55	35	7.1 ± 1.9

**70 °C-samples also contained around 300 ppm Fe, 200 ppm K, 20 ppm Mn and 10 ppm Zn, originate from the starting material, $CaCO_3$. The values in the $\%CO_3$ column were calculated from the experimental %C values. Carbon analyses were performed by using a LECO carbon analyzer (CS-200). Analyses (except those of particle size) of this table were performed only once.*

Notes

Certain commercial equipments, instruments, or chemicals are only identified in this article to foster understanding. Such identification does not imply recommendation or endorsement by the authors, nor does it imply that the equipment or chemicals identified are necessarily the best available for the purpose.

Acknowledgments

A.C. Tas was a visiting professor in the College of Dentistry at the University of Oklahoma Health Sciences Center (OUHSC) between October 1, 2010 and September 30, 2011, and a few of the characterization runs were performed there. Authors thank Ms. Lou Ann Miller of the Frederick Seitz Materials Research Laboratory of the University of Illinois at Urbana-Champaign for performing the DLS analyses.

References

[1] W.F. Neuman, M.W. Neuman, The Chemical Dynamics of Bone Mineral, University of Chicago Press, 1958.
[2] L.L. Hench, J. Wilson, An Introduction to Bioceramics, World Scientific, 1993.
[3] W. Castro, Elemental Analysis of Biological Matrices by Laser Ablation High Resolution Inductively Coupled Plasma Mass Spectrometry (LA-HR-ICP-MS) and High Resolution Inductively Coupled Plasma Mass Spectrometry (HR-ICP-MS), Ph.D. Thesis, Florida International University, Miami, Florida, 2008.
[4] S.V. Dorozhkin, Biphasic, triphasic and multiphasic calcium orthophosphates, Acta Biomaterialia 8 (2012) 963–977.
[5] D. Bayraktar, A.C. Tas, Chemical preparation of carbonated calcium hydroxyapatite powders at 37 °C in urea-containing synthetic body fluids, Journal of the European Ceramic Society 19 (1999) 2573–2579.
[6] A.C. Tas, Synthesis of biomimetic Ca-hydroxyapatite powders at 37 °C in synthetic body fluids, Biomaterials 21 (2000) 1429–1438.
[7] E. Landi, A. Tampieri, G. Celotti, R. Langenati, M. Sandri, S. Sprio, Nucleation of biomimetic apatite in synthetic body fluids: dense and porous scaffold development, Biomaterials 26 (2005) 2835–2845.
[8] M. Hashizume, Y. Nagasawa, T. Suzuki, S. Kawashima, M. Kamitakahara, Effect of preparative conditions on crystallinity of apatite particles obtained from simulated body fluids, Colloids and Surfaces B 84 (2011) 545–549.
[9] T.I. Ivanova, O.V. Frank-Kamenetskaya, A.B. Koltsov, V.L. Ugolkov, Crystal structure of calcium-deficient carbonated hydroxyapatite: thermal decomposition, Journal of Solid State Chemistry 160 (2001) 340–349.
[10] S. Kannan, F.G. Neunhoeffer, J. Neubauer, J.M.F. Ferreira, Ionic substitutions in biphasic hydroxyapatite and β-tricalcium phosphate mixtures: structural analysis by Rietveld refinement, Journal of the American Ceramic Society 91 (2008) 1–12.
[11] S. Pina, S.I. Vieira, P.M.C. Torres, F. Goetz-Neunhoeffer, J. Neubauer, O.A.B.D.E. Silva, E.F.D.E. Silva, J.M.F. Ferreira, In vitro performance assessment of new brushite-forming Zn- and ZnSr-substituted β-TCP bone cements, Journal of Biomedical Materials Research 94B (2010) 414–420.
[12] E. Hayek, F. Mullner, K. Koller, Zur Kenntnis des Hydroxylapatits, Monatshefte fur Chemie 82 (1951) 958–969.
[13] E. Hayek, J. Lechleitner, W. Bohler, Hydrothermal synthese von hydroxylapatit, Angewandte Chemie International Edition 67 (1955) 326.
[14] E. Hayek, H. Newesely, Pentacalcium Hydroxyorthophosphate, Inorganic Syntheses, vol. VII, McGraw-Hill, Inc., 1963, pp. 63–65.
[15] K. de Groot, Bioceramics consisting of calcium phosphate salt, Biomaterials 1 (1980) 47–50.
[16] M. Jarcho, C.H. Bolen, M.B. Thomas, J. Bobick, J.F. Kay, R.H. Doremus, HA synthesis and characterization in dense polycrystalline form, Journal of Materials Science 11 (1987) 2027–2035.
[17] R.Z. LeGeros, Calcium phosphate materials in restorative dentistry: a review, Advances in Dental Research 2 (1988) 164–180.
[18] M.A. Miller, M.R. Kendall, M.K. Jain, P.R. Larson, A.S. Madden, A.C. Tas, Testing of brushite ($CaHPO_4 \cdot 2H_2O$) in synthetic biomineralization solutions and in situ crystallization of brushite microgranules, Journal of The American Ceramic Society 95 (2012) 2178–2188.
[19] D.M. Roy, S.K. Linnehan, Hydroxyapatite formed from coral skeletal carbonate by hydrothermal exchange, Nature 246 (1974) 220–222.
[20] D.M. Roy, W. Eysel, D. Dinger, Hydrothermal synthesis of various carbonate-containing calcium hydroxyapatite, Materials Research Bulletin 9 (1974) 35–40.
[21] D.M. Roy, Porous Biomaterials and Method of Making Same, US Patent no.: 3,929,971, December 30, 1975.
[22] C.M. Zaremba, D.E. Morse, S. Mann, P.K. Hansma, G.D. Stucky, Aragonite-hydroxyapatite conversion in gastropod (abalone) nacre, Chemistry of Materials 10 (1998) 3813–3824.
[23] X.-W. Su, D.-M. Zhang, A.H. Heuer, Tissue regeneration in the shell of the giant queen conch, *Strombus gigas*, Chemistry of Materials 16 (2004) 581–593.
[24] M. Ni, B.D. Ratner, Nacre surface transformation to hydroxyapatite in a phosphate buffer solution, Biomaterials 24 (2003) 4323–4331.
[25] S. Jinawath, D. Polchai, M. Yoshimura, Low-temperature hydrothermal transformation of aragonite to hydroxyapatite, Materials Science and Engineering C 22 (2002) 35–39.
[26] J. Vuola, H. Goeransson, T. Boehling, S. Asko-Seljavaara, Bone marrow induced osteogenesis in hydroxyapatite and calcium carbonate implants, Biomaterials 17 (1996) 1761–1766.
[27] J. Vuola, R. Taurio, H. Goeransson, S. Asko-Seljavaara, Compressive strength of calcium carbonate and hydroxyapatite implants after bone marrow-induced osteogenesis, Biomaterials 19 (1998) 223–227.
[28] A.C. Tas, Porous, biphasic $CaCO_3$-calcium phosphate biomedical cement scaffolds from calcite ($CaCO_3$) powder, International Journal of Applied Ceramic Technology 4 (2007) 152–163.
[29] X. Long, M.J. Nasse, Y. Ma, L. Qi, From synthetic to biogenic Mg-containing calcites: a comparative study using FTIR microspectroscopy, Physical Chemistry Chemical Physics 14 (2012) 2255–2263.
[30] C. Rodriguez-Navarro, E. Ruiz-Agudo, A. Luque, A.B. Rodriguez-Navarro, M. Ortega-Huertas, Thermal decomposition of calcite: mechanisms of formation and textural evolution of CaO nanocrystals, American Mineralogist 94 (2009) 578–593.
[31] M. Anastasiou, T. Hasapis, T. Zorba, E. Pavlidou, K. Chrissafis, K.M. Paraskevopoulos, TG-DTA and FTIR analyses of plasters from Byzantine monuments in Balkan region, Journal of Thermal Analysis and Calorimetry 84 (2006) 27–32.
[32] G.N. Karagiannis, T.C. Vaimakis, A.T. Sdoukos, The effect of procedural variables and mechanical activation on the thermal decomposition of calcite. An approach by experimental design, Thermochimica Acta 262 (1995) 129–144.
[33] J. Garcia-Carmona, J. Gomez-Morales, J. Fraile-Sainz, R. Rodriguez-Clemente, Morphological characteristics and aggregation of calcite crystals obtained by bubbling CO_2 through a $Ca(OH)_2$ suspension in the presence of additives, Powder Technology 130 (2003) 307–315.
[34] K. Kadota, T. Yamamoto, A. Shimosaka, Y. Shirakawa, J. Hidaka, M. Kouzu, Aggregation modeling of calcium carbonate particles by Monte Carlo simulation, Journal of Nanoparticle Research 13 (2011) 7209–7218.
[35] E.I. Dorozhkina, S.V. Dorozhkin, Structure and properties of the precipitates formed from condensed solutions of the revised

simulated body fluid, Journal of Biomedical Materials Research 67A (2003) 578–581.
[36] A.C. Tas, S.B. Bhaduri, Rapid coating of Ti6Al4V at room temperature with a calcium phosphate solution similar to 10x simulated body fluid, Journal of Materials Research 19 (2004) 2742–2749.
[37] O. Suzuki, Octacalcium phosphate: osteoconductivity and crystal chemistry, Acta Biomaterialia 6 (2010) 3379–3387.
[38] C.K. Loong, C. Rey, L.T. Kuhn, C. Combes, Y. Wu, S.H. Chen, M.J. Glimcher, Evidence of hydroxyl ion deficiency in bone apatites: an inelastic neutron-scattering study, Bone 26 (2000) 599–602.
[39] Y. Suetsugu, Y. Takahashi, F.P. Okamura, J. Tanaka, Structure analysis of A-type carbonate apatite by a single-crystal x-ray diffraction method, Journal of Solid State Chemistry 155 (2000) 292–297.
[40] D. McConnell, Crystal chemistry of hydroxyapatite; its relation to bone mineral, Archives of Oral Biology 10 (1965) 421–431.
[41] J.C. Elliott, G. Bonel, J.C. Trombe, Space group and lattice constants of $Ca_{10}(PO_4)_6CO_3$, Journal of Applied Crystallography 13 (1980) 618–621.
[42] G. Bonel, Contribution to study of apatites carbonatation. 1. Synthesis and physicochemical properties of type A carbonated apatites, Annali di Chimica 7 (1972) 65–88.
[43] C. Rey, J.L. Miquel, L. Facchini, A.P. Legrand, M.J. Glimcher, Hydroxyl groups in bone mineral, Bone 16 (1995) 583–586.
[44] J. Li, Y. Li, L. Zhang, Y. Zuo, Composition of calcium deficient Na-containing carbonate hydroxyapatite modified with Cu(II) and Zn(II) ions, Applied Surface Science 254 (2008) 2844–2850.
[45] J.P. Lafon, E. Champion, D. Bernache-Assollant, Processing of AB-type carbonated hydroxyapatite $Ca_{10-x}(PO_4)_{6-x}(CO_3)_x(OH)_{2-x-2y}(CO_3)_y$ ceramics with controlled composition, Journal of the European Ceramic Society 28 (2008) 139–147.
[46] J.E. Barralet, S.M. Best, W. Bonfield, Carbonate substitution in precipitated apatite: an investigation into the effects of reaction temperature and bicarbonate ion concentration, Journal of Biomedical Materials Research 41 (1998) 79–86.
[47] R. Astala, M.J. Stott, First principles investigation of mineral component of bone: CO_3 substitutions in hydroxyapatite, Chemistry of Materials 17 (2005) 4125–4133.
[48] E.S. Kovaleva, M.P. Shabanov, V.I. Putlayev, Y.Y. Filippov, Y.D. Tretyakov, V.K. Ivanov, Carbonated hydroxyapatite nanopowders for preparation of bioresorbable materials, Materialwiss Werkst 39 (2008) 822–829.
[49] S. Kannan, A.F. Lemos, J.M.F. Ferreira, Synthesis and mechanical performance of biological-like hydroxyapatites, Chemistry of Materials 18 (2006) 2181–2186.
[50] G. Penel, G. Leroy, C. Rey, E. Bres, MicroRaman spectral study of the PO_4 and CO_3 vibrational modes in synthetic and biological apatites, Calcified Tissue International 63 (1998) 475–481.
[51] A. Antonakos, E. Liarokapis, T. Leventouri, Micro-Raman and FTIR studies of synthetic and natural apatites, Biomaterials 28 (2007) 3043–3054.
[52] M.E. Fleet, X.Y. Liu, X. Liu, Orientation of channel carbonate ions in apatite: effect of pressure and composition, American Mineralogist 96 (2011) 1148–1157.
[53] I.R. Gibson, W. Bonfield, Novel synthesis and characterization of an AB-type carbonate-substituted hydroxyapatite, Journal of Biomedical Materials Research 59 (2002) 697–708.
[54] J.B. Liu, K.W. Li, H. Wang, M.K. Zhu, H. Yan, Rapid formation of hydroxyapatite nanostructures by microwave irradiation, Chemical Physics Letters 396 (2004) 429–432.
[55] M.G. Ma, Y.J. Zhu, J. Chang, Monetite formed in mixed solvents of water and ethylene glycol and its transformation to hydroxyapatite, Journal of Physical Chemistry B 110 (2006) 14226–14230.
[56] K. Lin, J. Chang, Y.J. Zhu, W. Wu, G.F. Cheng, Y. Zeng, M.L. Ruan, A facile one-step surfactant-free and low-temperature hydrothermal method to prepare uniform 3D structured carbonated apatite flowers, Crystal Growth & Design 9 (2009) 177–181.